Radiation Physics and Chemistry xxx (xxxx) 114057

Contents lists available at ScienceDirect

Radiation Physics and Chemistry

journal homepage: www.elsevier.com/locate/radphyschem

Spectrometric and meteorological investigation of wind-induced gamma-ray storms (WiGRS)

A. Chilingarian *, B. Sargsyan

A. Alikhanyan National Lab (Yerevan Physics Institute), Yerevan, AM0036, Armenia

A B S T R A C T

Wind-induced gamma-ray storms (WiGRS) were observed during the 2024 winter monitoring campaign at Aragats (Chilingarian et al., 2025). In the present work, we provide the first spectrometric characterization of this phenomenon. Previous observations relied solely on integral gamma-ray count rates from SEVAN-type detectors (Chilingarian et al., 2018), which had low energy resolution at low energies (0.3-3 MeV), insufficient to resolve spectral lines of isotopes. Consequently, the physical origin of the enhancements could not be determined at the level of individual radionuclides. The present WiGRS observations differ fundamentally from previous results, combining precise spectrometric and meteorological observations to characterize this new regime and place it in the broader context of natural gamma-ray radiation variability. After installing a precise RT-56 gamma spectrometer in November 2025, we obtained the first full spectrometric characterization of WiGRS. The enhancement primarily originates from increased gamma-ray emission from long-lived terrestrial radionuclides, most clearly traced by K-40 and Tl-208, with a sustained U-series contribution consistent with Ra-226-bearing material brought by dust and soil during strong winds. Thus, the combination of high-resolution spectrometric data and meteorological measurements completes the physical interpretation of WiGRS, establishing it as a new source of NGR with parameters that are fundamentally different from those of the radon circulation effect in atmospheric electric fields.

Plain language summary

This paper examines unusual winter increases in natural gamma radiation recorded at the Aragats station. During strong winds and snowstorms, the gamma-ray count rate in a small laboratory ("Cuckoo's Nest") rises with wind speed. Using a gamma-ray spectrometer, we identify which naturally occurring radionuclides contribute to these increases and explain why the effect persists. In December 2025, when snow cover was thin and winds exposed soil and rocks, wind-borne mineral dust entered and settled inside buildings, causing a cumulative enhancement that persisted for several days. In contrast, the 2024 deep-snow event was short-lived and is consistent with radon and its short-lived decay products being pumped into the cabin through openings. We propose a practical definition and classification for these two WiGRS types to support reliable radiation monitoring and interpretation of winter data.

Key points

- Two distinct WiGRS subtypes are identified: a cumulative "dust-deposition" WiGRS (thin-snow conditions) and a "radon-pumping" WiGRS (deep-snow conditions).
- RT-56 spectrometry shows that wind-driven enhancement affects all discrete natural lines, with the strongest persistent growth in the 40K (1461 keV) and 208 Tl (2615 keV) lines.
- The cumulative WiGRS can persist for days and weeks after winds calm, and winter radiation background can remain elevated for a very long time, influencing highland and arctic/Antarctic environments.

CRediT authorship contribution statement

A. Chilingarian: Conceptualization, Investigation, Project administration, Supervision, Validation, Visualization, Writing – original draft. **B. Sargsyan:** Data curation, Formal analysis, Software, Validation.

* Corresponding author.
E-mail address: chili@aragats.am (A. Chilingarian).

https://doi.org/10.1016/j.radphyschem.2026.114057
Received 15 February 2026; Received in revised form 21 April 2026; Accepted 20 May 2026
0969-806X/© 20XX

1. Introduction

Natural gamma radiation (NGR) at the Earth's surface arises from primordial radionuclides in the crust (mainly U–Th series and K-40), cosmogenic components, and time-dependent contributions from atmospheric radioactivity and high-energy atmospheric processes (UNSCEAR, 2000). NGR modulation by snowpack and soil moisture is known from airborne gamma-ray snow surveys, where the gamma signal from K-40, -Th chains in the ground is attenuated by the overlying snow water equivalent (Carroll, 1980;.

Previous studies have shown that meteorological transport can significantly perturb natural radioactivity at mountain and polar stations. At Jungfraujoch in the Swiss Alps, radon observations demonstrated that boundary-layer air is intermittently transported to the high-altitude station by mountain winCds, measurably modifying the local atmospheric composition (Griffiths et al., 2014). In Antarctica, year-long high-precision observations at King Sejong Station on King George Island showed that ^{222}Rn is an effective tracer of terrestrially influenced air masses reaching the Antarctic environment (Chambers et al., 2014). More recently, long-term monitoring at the Polish Polar Station Hornsund showed that environmental gamma dose rate is significantly modulated by meteorological factors, especially snow depth and temperature (Nieckarz and Kubicki, 2025). These studies provide important context for weather-related perturbations of natural radiation backgrounds, but they do not appear to describe the present phenomenon: a high-mountain winter event spectrometrically resolved into a persistent enhancement of natural gamma-ray lines.

Gamma-ray monitoring at Aragats high-mountain stations has revealed that thunderstorm electric fields can strongly modulate NGR. Thunderstorm ground enhancements (TGEs, Chilingarian et al., 2010, 2011), abrupt enhancements of NGR during thunderstorms, are partly produced by gamma rays from radon progeny, primarily through the decay of 214 Pb and 214Bi isotopes (Chilingarian, 2018, 2019). By analyzing long-lasting TGEs during fair-weather recovery phases, these studies showed that the effective atmospheric half-life of the near-surface radon-progeny gamma component is about 20–25 min, consistent with the decay of short-lived daughters in the 222Rn chain (Chilingarian et al., 2019a, 2019b). Later, Chilingarian et al. (2020) demonstrated that near-surface electric fields (NSFs) can efficiently redistribute charged aerosols carrying radon progeny between the ground and cloud base, a process termed the “radon circulation effect”. In this framework, enhancements of NGR during TGEs are governed by a dynamic balance among exhalation from soil, vertical transport by electric fields, and radioactive decay. A comprehensive analysis of radon- and electric-field NGR sources in winter was presented by Chilingarian et al. (2021).

Wind-induced gamma-ray storms (WiGRS) were first identified during the 2024 winter NGR monitoring campaign at the Aragats high-mountain research station (3200 m a.s.l., Armenia). Strong winds mobilize Radon progeny and radionuclide-bearing particles, bringing them into proximity with detectors and indoor air volumes. Using SEVAN-type particle detectors, strong, long-lasting enhancements of gamma-ray count rates were observed during intense snowstorms, in the absence of thunderstorms (Chilingarian et al., 2025). SEVAN detectors (Chilingarian et al., 2018) provide integral count rates over a broad energy band; however, with an energy resolution of only 50–60% in the 0.3–3 MeV range, they are insufficient to resolve individual gamma-ray lines from specific radionuclides. Consequently, the initial WiGRS study identified the phenomenon as a new, wind-driven source of NGR. Still, it could not determine the isotopic composition of the emitted radiation and assumed that gamma radiation from Radon progeny was mostly responsible for WiGRS.

The present research with the precise spectrometers RT-56 indicates a fundamentally different origin of new phenomena. We observe that WiGRS enhancements, once initiated by strong winds, persist for many days, maintaining elevated count rates even after the wind speed decreases, in contrast to the 20–25-min decay tails characteristic of the half-lives of radon isotopes (214 Pb and 214Bi). Consequently, we show in this paper that WiGRS spectra are dominated by gamma-ray lines from 40K to 208 Tl, with a lower contribution from radon isotopes. Thus, spectrometric evidence clearly indicates that 2025 WiGRS represent a new type of NGR, not explained solely by free atmospheric radon-progeny transport, although radon daughters remain present through deposited parent material.

To obtain this spectrometric evidence, a high-resolution RT-56 NaI(Tl) gamma spectrometer was installed at Aragats in 2025, with SEVAN detectors and Davis weather stations. The RT-56 instrument provides high energy resolution in the sub-MeV range, allowing individual gamma-ray lines of natural isotopes to be resolved. Using Gaussian fits to the prominent peaks in background and storm-time spectra, we quantify the enhancements of the main natural radionuclides and identify the dominant contributors to different WiGRS episodes. In particular, we show that the most pronounced WiGRS events are associated with strong enhancements in the 1.46 MeV 40K line and the 2.61 MeV 208 Tl line.

In the context of earlier works, WiGRS can be interpreted as a cumulative, mechanically driven process: strong winds mobilize and transport aerosols and fine soil and snow particles that contain long-lived natural radionuclides. Because the half-lives of these parent radionuclides are extremely long, their activity does not decay on meteorological timescales; instead, the local gamma-ray field increases as more radioactive material is imported and deposited in buildings and detector housings. This explains why WiGRS maintain nearly constant intensities long after the wind has weakened, in sharp contrast to radon-dominated TGEs, whose intensity rapidly follows the 20–25-min effective atmospheric half-life of radon progeny.

The present spectrometric and meteorological investigation, therefore, serves two purposes. First, it completes the physical picture of WiGRS, demonstrating that they are produced mainly by long-lived natural radionuclides transported by wind rather than by short-lived radon progeny modulated by electric fields. Second, it highlights the broader importance of WiGRS for radiation monitoring and environmental modelling at high-altitude and polar stations, where strong winter winds and snowstorms are frequent. In such environments, WiGRS can become a dominant, cumulative contribution to NGR, persisting long after individual meteorological events and potentially biasing long-term background estimates unless they are properly identified and modeled.

2. Methodology

Gamma-ray spectra were recorded with an RT-56 spectrometer (Georadis s.r.o., Brno, Czech Republic) equipped with a large-volume NaI(Tl) scintillation detector (type 102B127/3M-X, Scionix Holland B.V., size 4x5”). The RT-56 spectrometer is a dual-range, pull-up spectrometer. Two identical spectrometers with different gains share the same input. The spectrometers' ranges are: Spectrometer A from 30 to 3000 keV, and Spectrometer B from 100 to 10,000 keV. Both spectrometers operate on 1024 channels. Spectrometer A uses two sets of 1024-channel vectors. The first, A1, serves for standard spectrum acquisition. The second, A2, performs spectrum integration in the background, regardless of the main spectrometer tasks. This spectrum is used to evaluate and measure peak-position drifts in the spectrum caused by a change in temperature. Any difference from the nominal position is corrected by readjusting the fine and coarse gain.

The NaI(Tl) light output as a function of the crystal temperature is determined by the material itself. The characteristic is parabolic, with maximum light output around 7 °C. Because of the permanent automated correction of drift, the RT-56 operates in the semi-linear area of the characteristic. The typical gain-temperature slope in this range is 0.12 %/°C. This corresponds to 26 keV/°C at an energy of 2615 keV. According to the manufacturer's specifications, the intrinsic resolution of the NaI(Tl) detector is ~ 7% at 662 keV when operated at a high voltage of +500-+900 V. In our configuration, the detector is interfaced

to the RT-series digital electronics from Georadis, which provide pulse-height analysis, 1024-channel acquisition, and online data transfer to the CRD database. The self-stabilization algorithm periodically evaluates the positions of peaks in the A2 spectrum and compares them with the expected pattern of naturally occurring radioactive materials (NORM) in the local background.

In previous SEVAN-light measurements, the detector consists of a 20 cm thick, 0.25 m^2 spectrometric scintillator with a 1 cm thick, 1 m^2 veto scintillator above it; it records energy-release histograms continuously, one per minute. Its LADC electronics cover 0.3–300 MeV but exhibit poor low-energy resolution in the lowest-energy band (60% at 662 keV), so it is not suitable for isotopic line spectroscopy.

WiGRS analysis is based on 24-h energy-release histograms spanning the pre-storm (Bg), storm (WiGRS), and post-storm intervals, during which isotope-specific enhancements were calculated. These spectrometric results are synchronized with 1-min wind-speed data from the co-located Davis weather station. The combined dataset allowed us to relate the 40K, 208 Tl, and radon-progeny lines to the strong winds.

2.1. Definition of WiGRS spectra and enhancement

We define two spectra accumulated over equal exposure time ΔT: a storm spectrum S(E), measured during the wind-induced gamma-radiation episode, and a quiet reference spectrum Bg(E), measured during a nearby period at calm-wind conditions. Both spectra are binned in deposited energy E (keV). The enhancement (difference – D) spectrum is computed bin by bin as

$$D(E) = S(E) - Bg(E).$$

Occasional negative values of D(E) due to Poisson fluctuations are discarded because a strictly positive quantity is required for logarithmic transformations. Unless stated otherwise, we use an energy interval of 50 keV–3 MeV for the total enhancement and 300 keV–3 MeV for isotope-line analysis to avoid the rapidly varying low-energy region, dominated by the detector threshold and strong multiple-scatter contributions (Compton continuum).

2.2. Energy resolution model and regions of interest definition

Isotope-specific contributions are quantified by integrating D(E) over fixed regions of interest (ROIs) around selected gamma lines. ROIs are defined in units of the Gaussian standard deviation $\sigma(E_0)$ of the detector response at the specific isotope line energy E_0. $\sigma(E_0)$ is obtained from a local fit of Bg(E) with a Gaussian peak plus a linear background term in a narrow neighborhood of E_0. For each line at nominal energy E_0, the integration window is

$$ROI(E_0) = [E_0 - 3\sigma(E_0),\ E_0 + 3\sigma(E_0)].$$

This choice captures the full Gaussian peak area essentially, while keeping the window sufficiently narrow to limit contamination from neighboring features.

2.3. Isotope-specific excess counts and relative enhancement

We focus on diagnostic lines corresponding to known isotopes listed in Table 2. We also checked for the anthropogenic Cs-137 isotope line. For each line energy E_0, we compute the integrated counts in the ROI for storm and background periods and define the net isotope excess as

$$N_{excess}(E_0) = N_{WiGRS}(E_0) - N_{Bg}(E_0) = \Sigma_{\ E \in ROI(E0)}\ D(E).$$

The isotope-specific enhancement relative to the background is then

$$100 \times N_{excess}(E_0) \ / \ N_{Bg}(E_0).$$

At each reference line energy, Bi-214 (609 keV), K-40 (1461 keV), Bi-214 (1764 keV), and Tl-208 (2615 keV), σ_{Bg} is obtained by fitting the corresponding peak in Bg(E) with a Gaussian plus a local linear term (Compton continuum). The continuum contribution to the enhancement is modeled as a smooth baseline C(E) fitted over the full energy band using a quadratic polynomial in energy. For each event, we also report the fractional contribution of each isotope line to the summed excess of the four selected lines.

2.4. Separation of smooth compton continuum from line excess

In addition to discrete photopeaks, the WiGRS enhancement spectrum contains a broad continuum caused by partial-energy deposition (primarily Compton scattering and multiple interactions). This continuum is present across the entire energy range, including beneath full-energy peaks. Therefore, the excess counts in a peak window generally include two contributions: (i) a genuine increase in the photopeak itself and (ii) a change in the continuum level within the same window.

To quantify these contributions consistently, we estimate a smooth, line-like baseline of the enhancement spectrum over 500 keV–3 MeV. The baseline is constrained to vary slowly with energy and is determined using robust smoothing so that narrow peak-like excursions are treated as outliers. In practice, the energy intervals around the selected gamma lines are excluded from influencing the baseline fit, ensuring that the baseline cannot reproduce photopeak shapes (“cannot eat peaks”). The resulting smooth curve represents the Compton-continuum enhancement C(E).

For each isotope line at energy E_0, we then evaluate the continuum contribution within the same ROI used for peak integration by integrating the baseline over that ROI (“Compton under the peak”). The line-only excess is obtained by subtracting this under-peak continuum contribution from the total excess measured in the ROI. We report both terms: the line-only excess (photopeak contribution) and the Compton-under-peak contribution (continuum contribution), which allows a fair comparison between events and between isotopes.

Table 2
Enhancement of marker-isotopes on 13-14 and 17 December 2025.

Isotope	Energy keV	FWHM keV	Background (counts)	13–14 Dec. line excess (counts)	13–14 Dec. line excess (%)	17 Dec. line excess (%)	17 Dec. line excess(counts)
Pb-214	352	28	1835785 ± 1355	399875 ± 632	21,8	28,3	519733 ± 721
Bi-214	609	49	1200949 ± 1096	251693 ± 502	21,0	28,6	343155 ± 586
Cs-137	662	53	not identified	-	-	-	-
Bi-214	768	61	776675 ± 881	126643 ± 356	16,3	23,4	182036 ± 427
Tl-208	911	73	700468 ± 837	116078 ± 341	16,6	24,5	171853 ± 415
Bi-214	1120	90	527498 ± 726	77015 ± 278	14,6	22,1	116664 ± 342
Bi-214	1238	99	425493 ± 652	54375 ± 233	12,8	19,9	84504 ± 291
Bi-214	1378	110	490406 ± 700	95182 ± 309	19,4	29,4	143962 ± 379
K-40	1461	117	490785 ± 701	102094 ± 320	20,8	31,0	152189 ± 390
Bi-214	1764	141	179308 ± 423	25560 ± 160	14,3	18,8	33770 ± 184
Bi-214	2204	176	109404 ± 331	27400 ± 166	25,0	27,5	30058 ± 173
Tl-208	2615	209	94235 ± 307	36316 ± 191	38,5	41,6	39159 ± 198

At energies above ~100 keV, Compton scattering becomes important, so many detected events deposit only part of the photon energy and populate a broad continuum rather than the full-energy peak. In the Cuckoo's Nest configuration, photons undergo additional scattering in surrounding materials (walls, snow, detector housing, cabin interior), shifting counts from full-energy peaks into the continuum (multiple scattering, degraded energy deposition). Photopeaks sit atop a continuum formed by Compton-scattering and backscatter components. Thus, all high-energy isotopes contribute to lower-energy isotope photopeaks. This makes recovery of genuine low-energy peaks very difficult. This is why we will use higher-energy markers with energies >0.5 MeV for WiGRS characterization and comparison, namely Bi-214 (609 keV), K-40 (1461 keV), Bi-214 (1764 keV), and Tl-208 (2615 keV).

3. Snow storm on 13-14 December and cumulative gamma-ray flux enhancement

3.1. Specific climatic conditions

A strong snowfall started at the Aragats high-mountain research station (3200 m a.s.l.) on 13 December 2025. In mid-December, the seasonal snow cover was still thin and discontinuous. During the storm, strong winds repeatedly removed loose snow from the station surroundings, exposing patches of soil and rock and enabling efficient resuspension of mineral dust (Fig. 1a). Two weeks later, on 27 December 2025, the first deep snow event deposited an approximately 50 cm layer and buried the exposed ground and roofs (Fig. 1b), suppressing dust uplift and strongly changing near-surface transport conditions. Thus, we analyze snowstorms represented by two 24-h spectra: on 13–14 December and 17 December 2025.

The measurements were performed in and around the Cuckoo's Nest laboratory at Aragats. The cabin (about 9 m^2) is elevated (≈8 m) and includes a pressure-equalization opening (≈15 cm diameter) in the floor to prevent structural damage during strong wind-driven pressure differences. The cabin houses particle detectors, including a plastic scintillator (25 cm thickness, 0.25 m^2 area) and an RT-56 gamma-ray spectrometer. Instrument masts at the cabin corners host a Davis weather station, an EFM-100 electric field mill, and all-sky cameras (see Chilingarian et al., 2024 for full site and instrumentation details).

Fig. 2 shows the 1-min time series of wind speed, near-surface electric field (NSEF), and RT-56 count rate starting on 12 December (UT). The onset of the storm is marked by a rapid increase in wind speed (up to about 20 m/s) and an abrupt rise in gamma-ray count rate. During the strongest gusts, the NSEF record is disturbed. This behavior is expected

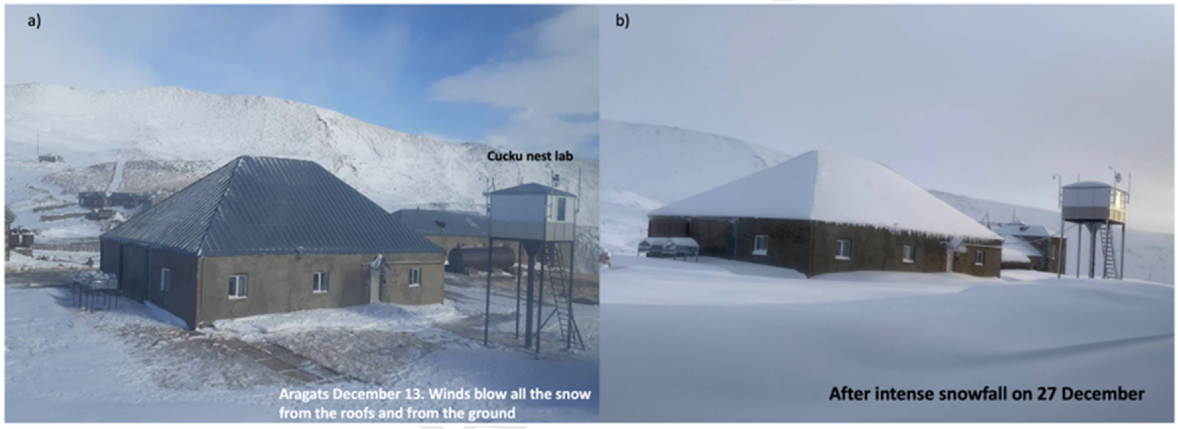

Fig. 1. SKL experimental hall and Cuckoo's Nest laboratory at Aragats station. (a) 13 December 2025: thin, wind-blown snow exposes ground and rocks, enabling dust resuspension. (b) 27 December 2025: first deep snow (≈50 cm) buries the ground and roofs, suppressing dust uplift (typical mid-winter conditions at 3200 m a.s.l.).

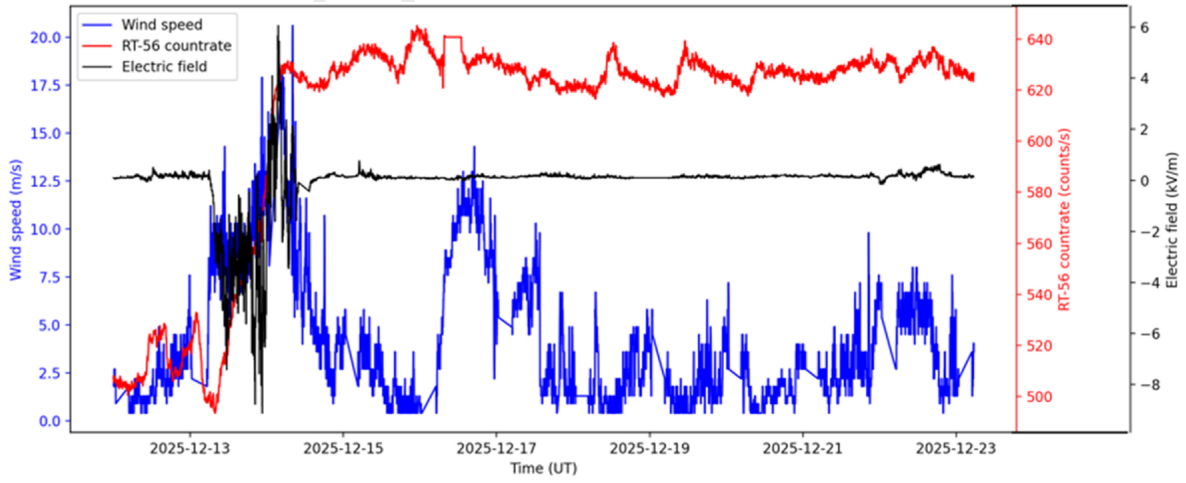

Fig. 2. Time series (1-min resolution) of wind speed (blue, left axis), RT-56 count rate (red, right axis), and near-surface electric field (black, right axis) starting on 12 December 2025 (UT). The wind onset coincides with an abrupt increase in gamma-ray count rate. NSEF disturbances during the storm are consistent with electric-field mill artifacts caused by electrified snow impacts and discharges. (For interpretation of the references to colour in this figure legend, the reader is referred to the Web version of this article.)

for electric-field mills during winter storms: dry, electrified snow and snow–ice fragments can strike the sensor plates, triggering transient electrical discharges that produce non-meteorological spikes and steps in the measured field (Chilingarian et al., 2024). Accordingly, NSEF variations during the storm should be treated as instrumental artifacts unless confirmed by independent field sensors or coherent behavior across multiple stations. In contrast to TGEs, no evidence here for a primary electric-field control is required or observed for WiGRS.

To reveal the source of the gamma-ray flux enhancement, we perform a detailed spectrometric analysis of the components of the overall gamma-ray enhancement in the next section.

3.2. Precise spectrometric information on long-lasting WiGRS

The key feature of the December 2025 event is its persistence: the gamma-ray flux remained elevated for more than 4 days after the wind weakened. Such long-lasting behavior is inconsistent with a purely radon-progeny-driven episode, because the short-lived daughters responsible for prominent radon-chain lines would decay within hours once ventilation and transport cease. The persistence instead points to the deposition and accumulation of long-lived radionuclides transported with wind-blown mineral material and retained within the station buildings. The separation between (i) long-lived, dust-borne components and (ii) short-lived radon-related components is established below using the RT-56 spectrograms.

To discriminate between these scenarios quantitatively, we analyze the RT-56 spectra to (i) separate the smooth Compton continuum from discrete line excess and (ii) quantify line-specific enhancements in fixed regions of interest centered on the isotope energies. The combined analysis enables us to distinguish between a cumulative, dust-driven WiGRS and a short-lived, radon-pumping WiGRS.

Figs. 3 and 4 present the WiGRS integrated for 24 h at the beginning of 13-14 December and on 17 December, 3 days later. Gamma-ray spectrograms with all major isotope lines were identified. This represents a detailed spectrometric demonstration that wind-driven gamma enhancements affect the entire natural radioactivity spectrum, although not uniformly.

The clearest lines in this band are the 40K line at 1461 keV and the 208 Tl line at 2615 keV, along with several lines of the U-series (radon progeny), notably 214Bi at 609 and 1764 keV and other visible 214Bi features across the spectrum. The fact that both the continuum and marker lines rise together provides direct spectrometric evidence that WiGRS impacts the full natural radioactivity spectrum recorded indoors.

The comparison between Fig. 3 (13–14 Dec) and 4 (17 Dec) supports the “cumulative” interpretation. The WiGRS–Bg separation is larger on 17 Dec than at the beginning of the storm, and this holds across the entire band, not just at a single energy. Therefore, the event does not simply “relax” after the wind peak; instead, the integrated effect increases over the subsequent days, consistent with deposition/accumulation within the building, which enriches indoor concentrations of long-lived isotopes.

In Table 1, we compare the overall gamma radiation enhancement at the beginning and after 3 days of the snowstorm. To quantify the overall WiGRS strength, including the low-energy portion of the RT-56 spectrum, the band-integrated enhancement is also evaluated over the 0.05–3 MeV range.

Thus, after 3 days, the gamma-ray radiation didn't decay but was even enhanced.

In Table 2, we present these enhancements for marker-isotopes. Table 2 shows the isotope name, energy, Full-width-on-half-maximum (FMHM), background, and identified peak counts and percent of enhancement relative to background for 24-h data files.

Wind transport on 13–14 Dec delivers and deposits dust and fine mineral particles enriched in K-bearing material (K-40), Th-series material (supporting Tl-208 at 2615 keV), and U-series material, including Ra-226. After deposition, the gamma activity can remain elevated for days to weeks because the parents (K-40, Ra-226, and Th-series parents) are effectively long-lived on the timescale of the campaign. Bi-214,609 and 1764 keV are short-lived daughters in the U-238 chain; therefore, a sustained many-day excess of these photopeaks during calm conditions is explained by transported and deposited mineral material containing the long-lived parent Ra-226 (half-life ≈1600 years).

Thus, WiGRS is a meteorology-driven radiological enhancement: increased flux of natural gamma emitters near the detector (dust/aerosols/deposition) raises the amplitudes of characteristic natural gamma lines. Anthropogenic Cs-137 isotope was not identified in the data samples.

The relative growth of isotopes increased over time as dust and mineral grains accumulated, were transported by wind, and were deposited in the Cuckoo's Nest cabin. Because the 214Bi lines remain elevated after three days, a purely short-lived “pumping-only” scenario (where activity is transported as airborne radon daughters and then stops) is insufficient.

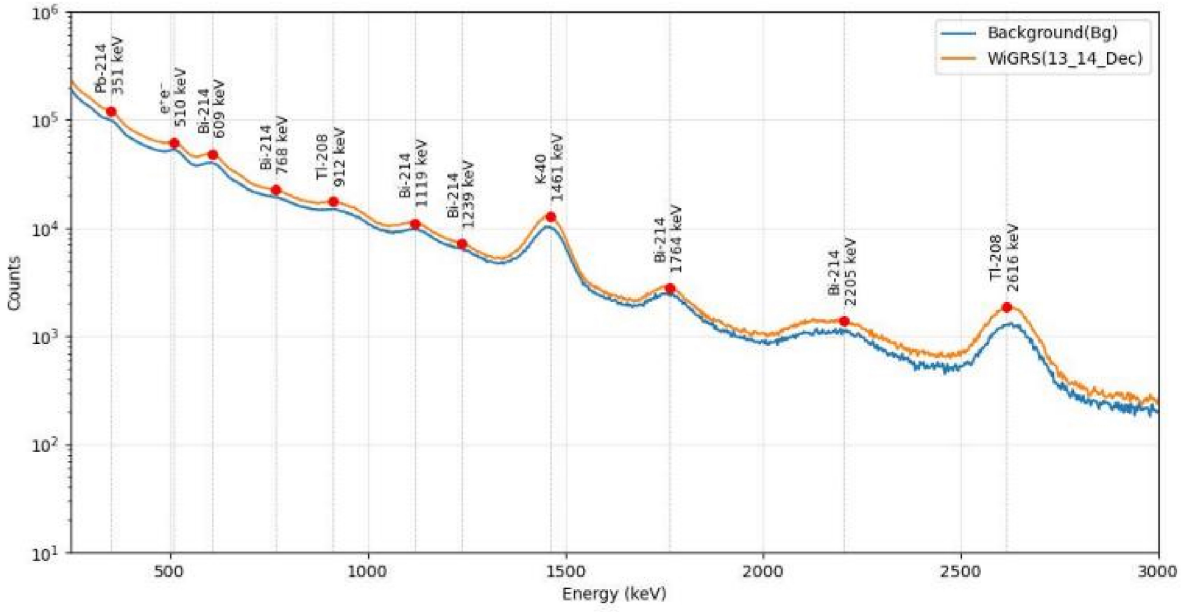

Fig. 3. 13-14 December (24 h): WiGRS and background (0.3 - 3 MeV) with identified lines.

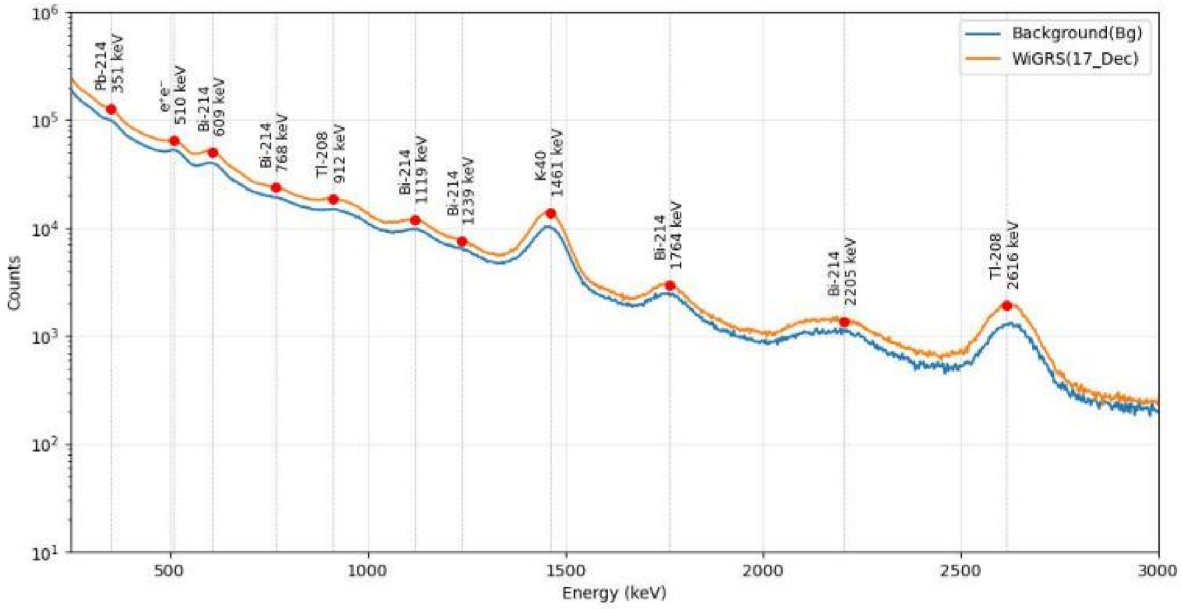

Fig. 4. 17 December (24 h): WiGRS and background (0.3 - 3 MeV) with identified lines.

Table 1
Overall radioactivity enhancement of the WiGRS event.

24 h interval	Bg counts (50–3000 keV)	Enhancement counts (50–3000 keV)	Relative enhancement (50–3000 keV) (%)	Relative enhancement (500–3000 keV) (%)
13–14 Dec	41,802,482	7,382,980	17.66	18.24
17 Dec	41,802,482	9,998,132	23.92	25.41

Persistence over days implies resupply by long-lived parents (e.g., the 226Ra-bearing mineral fraction), not free radon daughters alone. The consistent interpretation is that the storm introduces (or redistributes) long-lived parent material into the indoor environment, allowing continued generation of short-lived isotopes inside the building even when external winds weaken. This is exactly the physical distinction you emphasized between the 2024 “radon pumping under deep snow” event and the 2025 “thin snow + dust/deposition” event.

4. Deep-snow radon-pumping storm (Dec 2024)” versus “thin-snow ventilated plateau storm (Dec 2025)

The RT-56 WiGRS spectra (Dec 13–14 and Dec 17) show a stable dominance of K-40 (1461 keV) and Tl-208 (2615 keV) within the photopeak budget and a multi-day persistence, which is consistent with mineral material deposited near the detector (long-lived parents). By contrast, the deep-snow Cuckoo's Nest episodes in 2024 were dominated by radon progeny pumped from below; these produce very large but non-persistent enhancements that track ventilation conditions and wash out once pumping stops. This resolves the apparent discrepancy between the earlier ten-fold episodes and the current ~20% enhancements.

During the deep-snow period, there was no effective mineral-dust source at 3200 m, and the dominant mechanism was radon (Rn-222) exhalation from the ground/rock into the Cuckoo's Nest cavity, with wind-driven pumping through an opening in the floor. In this configuration, the observed gamma enhancement is expected to be dominated by the short-lived radon daughters (Pb-214, Bi-214), and it should rapidly diminish after pumping stops (minutes–hours), rather than persist for days–weeks as in the mineral-deposition WiGRS regime.

Evidence from the attached Cuckoo's Nest plastic scintillator dataset (25 cm thick, 0.25 m^2 area): the 30-min averaged count rate increases from a minimum of 233.1 to a maximum of 2529.7, i.e., a factor of 10.85 (≈10×), with the maximum at 2024-12-14 06:30 UTC (Chilingarian et al., 2025). The rise occurs during the interval of strongest winds, and the rate decreases afterward, consistent with a ventilation/pumping-controlled radon progeny contribution rather than deposition of long-lived mineral activity. The radiation enhancement (Fig. 2) persists elevated for days beyond the maximum wind speed at 5:00 UTC, 13 December. The mean count enhancement remains ≈21.4% over the next 4 days, consistent with a multi-day elevated level rather than a purely instantaneous pumping spike.

In Fig. 5, we compare the WiGRS detected with a 25 cm thick, 0.25 m area plastic scintillator located in the Cuckoo's Nest cabin. The small enhancement in 2025 (red curve) is not evident relative to the huge burst in 2024, so we zoom in on it in the inset. The multiday cumulative enhancement shown in the inset is drastically different from the impulse rise observed in 2024 (black curve).

5. Discussion

The spectrometric evidence presented here places WiGRS in clear contrast with previously studied natural gamma-ray phenomena. In earlier works, two complementary mechanisms of radon-related radiation were established. The first is the rapid vertical transport of radon progeny during thunderstorms, described by the radon-circulation mechanism (Chilingarian et al., 2020), which accounts for the strong enhancement of the Pb-214 and Bi-214 lines during TGEs. The second is the identification of an effective wind-pumping scenario based on the creation of radioactive electrified clouds following the half-lives of radon daughters (Chilingarian et al., 2025). These studies established that radon-driven natural gamma radiation is inherently self-limiting: once the electric field collapses, the excess activity decays exponentially with a characteristic lifetime of 20–25 min, reflecting the short physical half-lives of the Rn-222 progeny and the rapid removal of aerosols from the lower atmosphere.

The behavior of 2025 WiGRS is fundamentally different and cannot be explained by this radon-based framework. Because the dominant isotopes mobilized during WiGRS—K-40, Ra-226, and Tl-208—have extremely long nuclear half-lives, the radiation field remains sustained on meteorological timescales due to the continuous regeneration of short-lived daughters from long-lived parent material. Instead, WiGRS exhibits

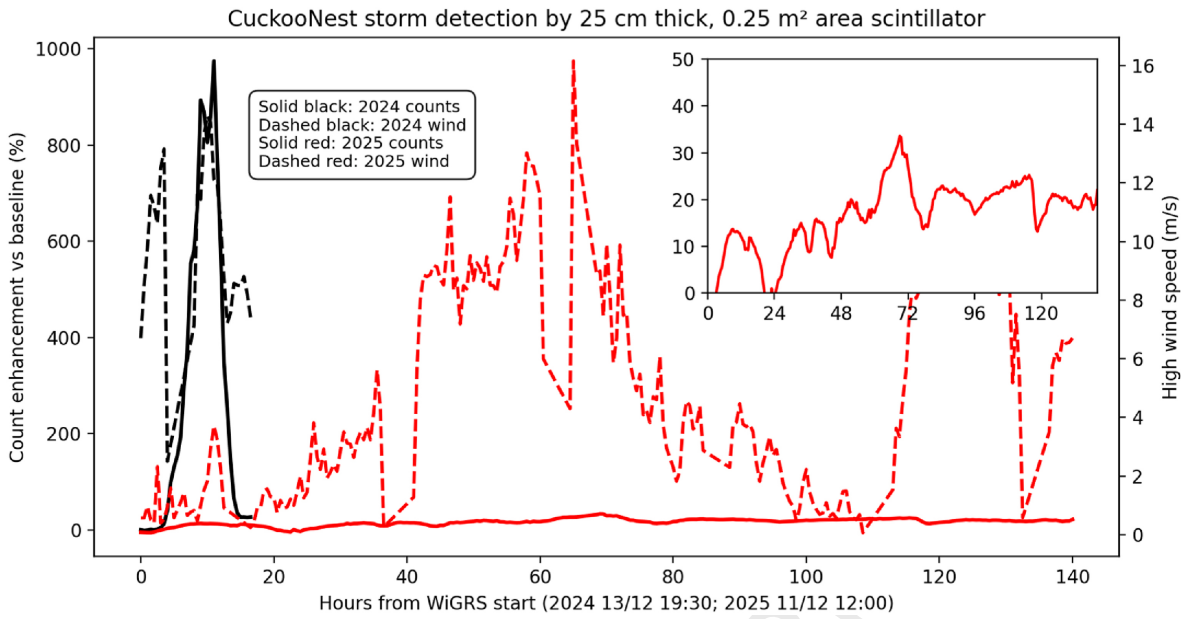

Fig. 5. Full-duration comparison of 2024 and 2025 WiGRS: enhancement vs. baseline and wind speed, with an inset zoom for 2025. Both time series are in relative time, with the wind rise as the starting point.

a cumulative character: as long as the wind continues to erode the snow surface and entrain soil particles, gamma-ray intensity can accumulate over several days. After the wind subsides, activity remains elevated for a prolonged period. This persistence reflects the residence time of soil-derived mineral dust in both indoor and outdoor environments, not the decay of radioactive isotopes. The contrast between the exponential decay of radon-based NGR and the quasi-stationary plateau of 2025 WiGRS therefore illustrates that different physical constraints govern these two phenomena—the former by the balance between radon influx and radioactive decay, the latter by the continuous injection and slow deposition of long-lived lithogenic nuclides.

The dominance of K-40 and Tl-208 in the 2025 WiGRS spectrum suggests that wind-driven natural gamma radiation represents a distinct environmental process that has not been previously resolved in the literature. Although numerous studies have reported correlations between meteorology and ambient gamma dose—typically linked to radon exhalation, aerosol washout, or atmospheric stability (Takeyasu et al., 2006)—none have documented large, rapid enhancements of K-40 and Th-chain gamma lines associated with wind erosion of soil at high altitudes. Research on snow-attenuation gamma techniques recognizes that snow redistribution modifies K-40 and Th-series signals, but these studies do not treat wind-induced gamma-ray enhancements as a distinct atmospheric radiation phenomenon (Tchorz-Trzeciakiewicz et al., 2023).

Thus, within the current state of knowledge, the data presented here constitute the first detailed spectrometric identification of a new form of natural gamma radiation driven by strong winter winds. The existence of this mechanism has important implications for environmental radiation monitoring at mountain research sites, where thin snow cover and exposed surfaces can lead to sudden increases in gamma background unrelated to radon or electrical atmospheric activity. It also expands the classification of natural gamma-ray events: wind-driven WiGRS must now be considered alongside radon-driven TGEs and thunderstorm-related particle accelerators as an independent contributor to variability in high-mountain radiation.

Declaration of competing interest

The authors declare that they have no known competing financial interests or personal relationships that could have appeared to influence the work reported in this paper.

Acknowledgment

We thank the staff of the Aragats Space Environmental Center for the uninterrupted operation of all particle detectors under severe winter conditions. The authors acknowledge the support of the Science Committee of the Republic of Armenia (Research Project No. 21AG-1C012) in modernizing the technical infrastructure of high-altitude stations.

Glossary

Natural gamma radiation (NGR) Natural gamma radiation denotes the near-surface gamma-ray field measured by ground-based detectors and produced by terrestrial radionuclides (crustal 40K and the U/Th series), atmospheric radon (Rn-222) and its progeny attached to aerosols, and their associated Compton continua in the detector response. In addition, during thunderstorms, NGR can be supplemented by gamma rays generated in the atmosphere by high-field acceleration processes, observed at ground as thunderstorm ground enhancements (TGEs).

Thunderstorm ground enhancement (TGE)A TGE is a short-lived enhancement of electrons and gamma rays produced by particle acceleration in thundercloud electric fields. TGEs are defined by a strong atmospheric electric-field configuration and their characteristic impulsive/episodic time structure, and they are not contingent on wind-driven transport of radioactive material.

Wind-induced gamma-ray enhancements (WiGRS) WiGRS are strong, long-lasting enhancements of NGR observed during dry snowstorms with intense wind under subzero temperatures, in the absence of thunderstorm-related electric-field conditions. In WiGRS, the measured spectrum below 3 MeV remains dominated by natural radionuclide lines and their Compton continua. At the same time, the enhancement persists for hours and can extend to multi-day increases in fluence and dose.

Two mechanistic subtypes of WiGRS.

The same observational class (WiGRS) can arise from at least two physically distinct transport regimes. For clarity, we distinguish:

(i) Radon-pumping WiGRS (RP-WiGRS)This subtype occurs when radon-rich air and its short-lived progeny are transported or accumulate near the detector by ventilation (“wind pumping”)

through cavities, building openings, or subsurface pathways, particularly under deep-snow conditions that suppress direct mineral-dust input. Spectroscopically, RP-WiGRS are characterized by enhanced radon progeny lines (notably 214Bi at 609 and 1764 keV) and rapid decay once pumping or ventilation is reduced, consistent with the short half-lives in the Rn-222 decay chain. This subtype produces large but typically non-persistent enhancements once the pumping pathway closes or mixing changes.

(ii) (ii) Dust-driven WiGRS (DT-WiGRS)This subtype occurs when strong winds and blowing snow mobilize and redeposit mineral aerosols or fine debris from exposed rocks/ground near the site (with thin snow cover or exposed terrain). In this regime, the enhancement can persist for days because the local radioactive environment around the detector is modified by deposited material containing long-lived parents in the U/Th series and 40K-bearing minerals. Spectroscopically, DT-WiGRS tend to show a comparatively stronger contribution of the 40K (1461 keV) and 208 Tl (2615 keV) photopeaks within the line budget, together with an elevated Compton continuum, while radon progeny lines may be weaker if radon exhalation and attachment are not concurrently enhanced.

Data availability

Data will be made available on request.

References

Carroll, T.R., 1980. Airborne gamma snow surveys and snow water equivalent modeling. Nordic Hydrology 11, 51–62.

Chambers, S.D., Hong, S.-B., Williams, A.G., et al., 2014. Characterising terrestrial influences on antarctic air masses using Radon-222 measurements at King George Island. Atmos. Chem. Phys. 14, 9903–9916. https://doi.org/10.5194/acp-14-9903-2014.

Chilingarian, A., 2018. Long lasting low energy thunderstorm ground enhancements and possible Rn-222 daughter isotopes contamination. Phys. Rev. D 98, 022007.

Chilingarian, A., 2019. Reply to "Comment on 'Long lasting low energy thunderstorm ground enhancements and possible Rn-222 daughter isotopes contamination' ". Phys. Rev. D 99, 108102. https://doi.org/10.1103/PhysRevD.99.108102.

Chilingarian, Avetisyan, A., Hovsepyan, G., Karapetyan, T., Kozliner, L., Sargsyan, B., Zazyan, M., 2019b. Origin of the low-energy gamma ray flux of the long-lasting thunderstorm ground enhancements. Phys. Rev. D 99, 102002.

Chilingarian, A., Aslanyan, D., Sargsyan, B., 2021. On the origin of particle flux enhancements during winter months at aragats. Phys. Lett. 399, 127296. https://doi.org/10.1016/j.physleta.2021.127296.

Chilingarian, A., Aslanyan, D., Sargsyan, B., Kozliner, L., 2025. Wind-induced natural gamma radiation. EPL (Europhysics Letters) 151, 14001. https://doi.org/10.1209/0295-5075/ade562.

Chilingarian, A., Daryan, A., Arakelyan, K., Hovsepyan, G., Mailyan, B., Melkumyan, L., et al., 2010. Ground-based observations of thunderstorm-correlated fluxes of high-energy electrons, gamma rays, and neutrons. Phys Rev D 82, 043009.

Chilingarian, A., Hovsepyan, G., Elbekian, A., et al., 2019a. Origin of enhanced gamma radiation in thunderclouds. Phys. Rev. Res. 1, 033167, 2019.

Chilingarian, A., Karapetyan, T., Sargsyan, B., Khanikyanc, Y., Chilingaryan, S., 2024. Measurements of particle fluxes, electric fields, and lightning occurrences at the aragats space-environmental Center (ASEC). Pure Appl. Geophys. 181, 1963. https://doi.org/10.1007/s00024-024-03481-5.

Chilingarian, A., Sargsyan, B., Hovsepyan, 2020. Circulation of radon progeny in the terrestrial atmosphere during thunderstorms. Geophys. Res. Lett. 47. https://doi.org/10.1029/2020GL091155. PRE.

Chilingarian, Babayan V., Karapetyan, T., et al., 2018. The SEVAN worldwide network of particle detectors: 10 years of operation. Adv. Space Res. 61 (10), 2680–2690. https://doi.org/10.1016/j.asr.2018.02.030.

Griffiths, A.D., Conen, F., Weingartner, E., et al., 2014. Surface-to-mountaintop transport characterized by radon observations at the Jungfraujoch. Atmos. Chem. Phys. 14, 12763–12779. https://doi.org/10.5194/acp-14-12763-2014.

Nieckarz, Z., Kubicki, M., 2025. Influence of meteorological and cosmic conditions on dose rate in the environment of the Polish Polar station Hornsund. Int. J. Biometeorol. 69, 2941–2951. https://doi.org/10.1007/s00484-025-02999-0.

Takeyasu, M., Iida, T., Tadashi, Tsujimoto T., et al., 2006. Concentrations and their ratio of 222 Rn decay products in rainwater measured by gamma-ray spectrometry using a low-background Ge detector. J. Environ. Radioact. 88 (2006), 74. https://doi.org/10.1016/j.jenvrad.2006.01.001.

Tchorz-Trzeciakiewicz, D.E., Kozłowska, B., A. Walencik-Łata, A., 2023. Seasonal variations of terrestrial gamma dose, natural radionuclides and human health. Chemosphere 310, 136908. https://doi.org/10.1016/j.chemosphere.2022.136908.

United Nations Scientific Committee on the Effects of Atomic Radiation (UNSCEAR), 2000. Sources and Effects of Ionizing Radiation: UNSCEAR 2000 Report to the General Assembly, with Scientific Annexes. Volume I: Sources. United Nations, New York.